Journal of Metals, Materials and Minerals, 35(2), e2218, 2025

Electrochemical study of Zn-Fe alloy coatings on mild steel for automotive applications

Ramesh S. BHAT[1,*], and A. CHITHARANJAN HEGDE[2]

[1] *Department of Chemistry, NMAM Institute of Technology, NITTE (Deemed to be University), Nitte -574110, India*
[2] *Electrochemistry Laboratory, Department of Chemistry, National Institute of Technology Karnataka, Srinivasnagar, 575025 India*

***Corresponding author e-mail**: rameshbhat@nitte.edu.in

Received date:
1 December 2024
Revised date:
4 April 2025
Accepted date:
22 April 2025

Keywords:
Electrodeposition;
Corrosion additive;
Surface morphology;
Micro-strain

Abstract

This study investigates the electrochemical behavior of Zn-Fe alloy deposited on mild steel (MS) substrates for automotive applications. The electrodeposition of a Zn-Fe alloy onto MS using an acid chloride bath, with 1,2,4-Triazole as an additive to enhance the uniformity of the deposit. The hull cell method was used to optimize the bath composition and operating conditions. The coatings were produced using electrodeposition at varying current densities, with 3 $A \cdot dm^{-2}$ identified as the optimal current density (CD) for achieving uniform coatings. The microstructural properties, including crystallite size and micro-strain, were analyzed using X-ray diffraction (XRD) and Williamson-Hall (W-H) analysis, revealing a homogenous distribution of crystallite size and strain. The impact of CD on coating features such as hardness, cathode current efficiency (CCE), thickness, and the weight % of metal contents was investigated. The corrosion resistance of the deposit was estimated using the potentiodynamic polarization and electrochemical impedance spectroscopy methods, and the results have been discussed. The structural and morphological properties of the deposit were investigated by Scanning electron microscopy (SEM). The roughness of the deposit was studied by Atomic force microscopy (AFM). The deposits containing Zn and Fe contents were confirmed by Energy-dispersive spectroscopy (EDS). The results suggest that Zn-Fe alloy coatings can provide superior protection for automotive components.

1. Introduction

Metals such as mild steel and cast iron are extensively used in construction and machinery due to their structural properties and affordability. However, these metals often face exposure to harsh environments where corrosion resistance (CR) is a significant concern, particularly when high uniformity is required. While mild steel and similar low-cost alloys offer some degree of corrosion resistance, their limited durability can restrict their use in more demanding applications [1]. Zinc coating, commonly referred to as galvanization, is a widely used method for protecting steel through sacrificial protection. This coating acts as a defensive layer, preventing corrosion of the underlying metal, and is favoured for its cost-effectiveness and versatility. Galvanized products are prevalent in various applications, including roofing sheets, fasteners like bolts, nuts, and screws, as well as washers [2]. In the pursuit of enhancing CR and extending the lifespan of industrial products, there is an increasing demand for protective coatings that can withstand hazardous environments, thereby supporting a more sustainable society. It is well-established that incorporating iron-group metals such as cobalt (Co), iron (Fe), and nickel (Ni) into zinc plating can significantly improve corrosion resistance [3-5].

Zn alloy electroplating, including Zn-cobalt and Zn-iron, has garnered significant attention due to its markedly improved CR compared to pure Zn coatings. These alloys serve as promising alternatives to harmful and costly cadmium electroplates [6-8]. The process of electrodepositing metals (EM) and alloys is widely utilized across various industries, such as automotive and defence, due to its distinct advantages over other metal finishing technologies [9]. These benefits include better control over coating properties, cost-effectiveness, and the ability to tailor surface characteristics to meet specific application requirements. Zn and Zn-M (Ni, Co, Fe) alloy plating are among the most effective and straightforward techniques for achieving robust corrosion protection. This method is widely utilized for electroplating Zn with Fe-group metals, offering an efficient way to enhance the durability of various components. Zn-Fe alloy coatings deliver exceptional CR and paint adhesion, making them highly suitable for a range of chemical and galvanic processes in the automotive and aerospace industries [10-12]. Using steady-state polarization (SSP) techniques, the behavior of Zn, Fe, and Zn-Fe deposited on Cu substrate from chloride baths containing ethylene-diamine tetra-acetic acid (EDTA) and boric acid was examined [13]. Also, in alloys with a small wt% of Fe in the plating, R. S. Bhat *et al.* [14] revealed that the presence of different additives in the electrolytic bath improves the surface uniformity and CR. The electrodeposition of Zn alloys on steel substrate provides significant corrosion protection [15-19]. Although the production of zinc alloys with additional metals, mainly transition metals like Cu, Fe, Ni, Co, and Mn, can minimize the corrosion of steel, the corrosion stability and endurance of these binary alloys are insufficient to provide the entire protection. It is generally known that Zn-M (Ni, Fe, and Co) alloys electrodeposition follows the irregular co-deposition type, with zinc deposition taking precedence over other nobler metals used in alloy productions, which may offer them a distinguishing feature, and thus their alloys have recently attracted great interest [20,21]. In comparison to single metal

plating, Eliaz *et al*. [22] found that deposition of Zn-Fe group metals confirmed improved CR. A. Toghan *et al*. [23] explained the detailed electrodeposition and corrosion mechanism. Electrodeposited Zn-Fe coatings on mild steel present a cost-effective solution for enhancing corrosion protection, significantly improving CR, and enhancing mechanical properties. These coatings offer an eco-friendly alternative to toxic cadmium (Cd) coatings, which have traditionally been used for corrosion protection [24,25]. Surfactants play a crucial role in the electrolysis process, influencing the quality of the deposited coating. The incorporation of cetyltrimethylammonium bromide (CTAB) into the electrolysis bath is particularly beneficial. CTAB, a cationic surfactant, helps in the efficient removal of hydrogen during deposition, resulting in a smoother and more uniform coating with enhanced brightness. Additionally, CTAB functions as both a corrosion inhibitor and a brightener, further improving the quality and protective properties of the alloy coatings [26]. It is well established that appropriate surface modification can significantly enhance the CR of metal or alloy systems.

In the present study, a new approach of Zn-Fe coating was proposed and examined to improve the corrosion resistance of Zn-Fe alloy coatings on MS using 1,2,4-triazole as an additive. The surface topography of the coating was analyzed by SEM. The phase structure of the coating was confirmed by XRD analysis. The roughness of the coating was confirmed by AFM. The study focused on analysing the effects of applied CD on various characteristics of the Zn-Fe coating, including its composition, phase structure, cathode current efficiency (CCE), thickness, hardness, roughness, morphology, and resistance to corrosion. These parameters were thoroughly investigated to understand how 1,2,4-triazole influences the performance and durability of the Zn-Fe alloy coating.

2. Experimental

2.1 Surface cleaning mild-steel

The MS sheets, each measuring 3 cm × 2 cm, were polished to a smooth finish using sandpaper with varying grit sizes (100, 180, 360, 500, 800, 1200, and 2000). To expose only 5 cm^{-2} of the substrate, a copper wire was soldered to the back of each sheet, and the remaining area was sealed with epoxy resin. The substrates were then washed with acetone before undergoing electro-cleaning. In this process, each MS sheet was cathodically cleaned in a degreasing bath at room temperature by passing a 1 A cell current through a platinum foil anode for 10 min. This step was crucial for removing oxides, oil, and other contaminants. After cleaning, the MS sheets were thoroughly rinsed with purified water and dried [27].

2.2 Optimization of electrolyte

The new chloride bath has been optimized for uniform Zn-Fe deposition on MS substrate. 1,2,4 triazole was used as an additive for the brightness of the deposition. The influence of electrodeposition bath and working parameters, on deposit characters and their anti-corrosion behaviors, were studied. All coating films were carried out at 30°C, fixed pH (3.0), and showed good reproducibility. The plating bath was made with de-ionized water and research-grade chemicals. The Hull cell method was employed, and the 1 A cell current passed for 5 min to optimize the bath components and operating parameters [28]. Polished MS was the cathode (5 cm^{-2}), while pure Zn served as the anode. All electroplating films were done galvanostatically using a direct current (DC) energy source, (N6705C, Key sight Technologies) for 10 min for assessment of coating purposes. The composition of each component was altered, and deposits were analyzed. The composition of the bath and the ACD have been adjusted based on appearance and CR. The effect of the addition of ETC and other bath constituents was varied. A range of ACDs 1.0 $A{\cdot}dm^{-2}$ to 5.0 $A{\cdot}dm^{-2}$ was used to produce a variety of deposits like burnt/bright/greyish appearance. The surface smoothness (visual observation) and uniformity of the deposits, the bath compositions arrived at optimization were: 25 $g{\cdot}L^{-1}$ Zinc chloride ($ZnCl_2$), 15 $g{\cdot}L^{-1}$ Ferrous chloride (FeCl2), 10 $g{\cdot}L^{-1}$ Boric acid (H_3BO_3), 5 $g{\cdot}L^{-1}$ citric acid, and 2 $g{\cdot}L^{-1}$ 1,2,4 triazole, and have been proposed for the fabrication of Zn-iron coating films on MS substrate.

2.3 Zn-Fe coating and its characterizations

For the electrodeposition, zinc is an anode, and MS acts as a cathode. Before the electrodeposition, the polished MS plates were washed with distilled water. For electroplating, the 50 mL capacity of the electrolytic cell was utilized, with an anode-cathode gap of 5 cm, which was necessary to minimize the voltage drop in the setup. After deposition, the substrate was cleaned with deionized water and dried. A potentiostat (CH instrument), in a three-electrode cell, (MS plate as a working, calomel as a reference, and platinum as a counter electrode), the corrosion test was performed. 5% NaCl was used as a corrosion medium for this study. The PP experiment was done with a theoretical potential ramp of ± 200 mV about the open circuit potential (OCP) at a scanning rate (SR) of 0.1 $m{\cdot}Vs^{-1}$. At various applied CDs, the corrosion current (i_{corr}), and corrosion potential (E_{corr}) were determined. The Nyquist plot was used to examine the electrochemical impedance behavior of the deposits at various applied CDs in the range of frequency 100 kHz to 10 MHz. The weight percent of Fe content in the deposit was estimated calorimetrically [29] and double-checked using the EDS technique. The thickness of the deposits was estimated from Faraday's Equation:

$$t = \frac{(E \times I_c \times CE \times \Delta T}{D \times F}$$

where t is the thickness of the deposit, E is the equivalent weight, I_C is the current density of the deposit, CE is current efficiency, ΔT is time, D is the coating density, and F is Faraday's constant (96,500 Coulombs). The calculated thickness was cross-checked with a digital thickness tester (coat-measure). The deposit hardness (~20 μm) was determined by the Vickers Hardness instrument at a weight of 500 g for 10 s at ambient temperature (30°C). 10 measurements were taken for each sample. The CCE of the coating was estimated by using the mass and composition of the coating [30]. An XRD (Bruker AXS) with Cu K- radiation (1.5405 = Å, 30 kV) was used to analyze the phase structure of the deposit. SEM (JSM-6380 LA from JEOL, Japan) was used to analyze the microstructure of the deposit. AFM (Nano-surf Flex AFM, Switzerland) was used to determine the roughness of the deposit.

3. Results and discussion

3.1 Influence of applied CD

From the optimized bath, Zn-Fe alloy deposits were prepared by direct current (DC). In alloy depositions, the CD has a prominent role in the structure, and properties, composition. The depositions were carried out at different CDs (1.0 A·dm^{-2} to 5.0 A·dm^{-2}) and were characterized by subjecting them to different tests. Table 1 displays the results of applied CD on Fe content, hardness, CCE, and thickness of the deposit. The bath produced a greyish deposit with 1.37 wt% Fe at low CD, and at high CD; the bath produced a porous bright deposit with 7.9 wt% Fe (Table 1). A smooth and crack-free deposit was found at 3.0 A·dm^{-2} (optimal CD) with 3.10 wt% Fe. An increase in the Fe content with CD is due to the sudden reduction of more readily depositable Zn^{+2} ions at the cathode [14,21,31].

In all ACDs, the CCE of the bath was high, which is greater than 87.3% (Table 1). CCE was increased with CD to an optimal value. In general, a slight decrease in CCE with increasing CD was observed, which could be related to excessive hydrogen evolution during electrodeposition. The increase in hardness and Fe content of the coatings with increase in CD (Table 1) and may be due to the high density of Fe. The deposit was bushy and porous, with improved hardness, at a high CD. The CD was found to show a direct relationship with deposit thickness (Table 1). It was observed that the linear dependence of thickness with CD, due to the adsorbed hydroxide of metal at the cathode, is caused by an increase in pH due to the hydrogen evolution [9,14,32].

3.2 Effect of agitation

The agitation is an important aspect of the chemical process, particularly in electrodeposition. Agitation of an alloy plating bath can directly affect the Fe content and its surface appearance (Table 2). This is a mechanical action that does not affect the electrochemical characteristics of the bath. The agitation has a more consistent effect on wt% Fe in the deposit, then either temperature or ACD [33]. As a result, the entire Zn-Fe electroplating process was carried out under constant agitation. The results show that the drop in iron content with agitation is due to the more eagerly Zn deposited on the cathode. Further, the appearance of the deposit turned greyish-white at high agitation due to an increase in Zn content.

3.3 Potentiodynamic polarization analysis (PP)

The CR of electrically plated Zn-Fe alloy onto the MS was investigated using the PP technique at room temperature with varied plating CDs as shown in Figure 1 (only representative). The corrosion CD (i_{corr}) and corrosion potential (E_{corr}) of the coatings are shown in Table 3. The increase of i_{corr} with CD may be due to the change in the structure of the deposits caused by high Fe content in the coating. The values of Tafel slopes indicate that a cathodic reaction controls the CR more than an anodic reaction (Figure 1). Further, it was found that the deposit at 3.0 A·dm^{-2}, electroplated Zn-Fe coating having 3.10 wt% Fe exhibits the least i_{corr} (14.51 µA·cm^{-2}), as shown in Table 3 and showing the peak CR [14,21].

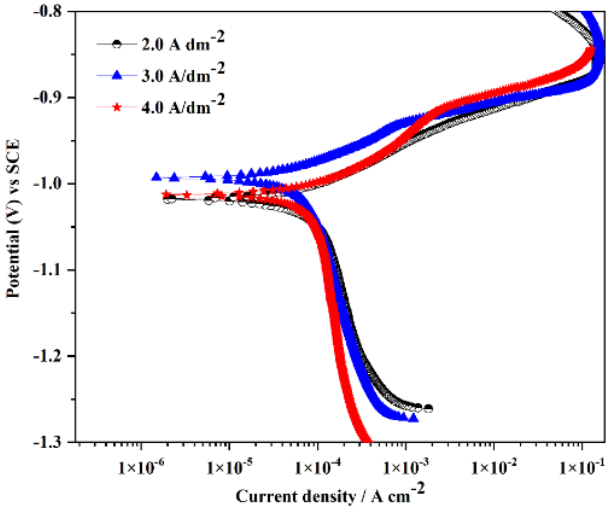

Figure 1. The potentiodynamic polarization curve of Zn-Fe coating films.

Table 1. The effect of ACD on the deposit characteristics of Zn-Fe alloy coatings from an optimum bath.

CD *i* [A·dm^{-2}]	pH of bath	Fe [wt%]	CCE [%]	Hardness (VH_{500})	*t* [µm]	Nature of deposit
1. 0	3.0	1.37	87.3	125	12.9	Greyish
2. 0		2.27	90.5	146	15.5	Semi bright
3. 0		3.10	93.1	158	18.2	Bright
4.0		5.70	92.8	162	21.1	Bright
5.0		7.90	91.9	169	23.5	Porous bright

Table 2. Result of agitation on wt% Fe content in the coating at 3.0 A·dm^{-2} and pH 3**.**

Agitation [rpm]	Fe [wt%]	Appearance of the deposit
0	4.56	Blackish
100	3.98	Grayish
500	3.10	Bright
1000	2.25	Grayish bright
1500	1.01	Grayish white

Table 3. Corrosion data of deposited Zn-Fe alloy from an optimum bath in 5% sodium chloride under various ACDs.

ACD i [A·dm^{-2}]	$-E_{corr}$ (V vs. Calomel)	i_{corr} [μA·cm^{-2}]
1.0	1.019	22.26
2.0	1.017	15.98
3.0	0.989	14.51
4.0	1.014	16.30
5.0	1.132	25.71

It may also be noted that the E_{corr} value of coated Zn-Fe (–0.989 V) at 3 A·dm^{-2} is more negative than MS (–0.774), evidencing the sacrificial protection of the deposit. As a result of proper complexation, the addition of 1,2,4 triazole to the plating bath has reduced the free Fe^{+2} ions in the plating bath, enhancing deposit uniformity and increasing corrosion resistance [14].

3.4 Electrochemical impedance spectroscopy (EIS) study

EIS has shown to be a beneficial tool for electrochemical systems, such as corrosion and batteries. Because it has many advantages over direct current (DC) electrochemical techniques and can provide you with a lot of information about the system being studied. The electrode response is likewise in a linear potential band because of the little fluctuation of AC signals, protecting the electrode from destruction. EIS is a powerful method for examining the electrical properties of materials, as well as the interfaces of conducting electrodes, in a variety of research areas because it can be used to assess the sequential relationship between interface characteristics [31,32]. As a result, the corrosion behavior of Zn-Fe coatings developed at CDs (1 A·dm^{-2} to 5 A·dm^{-2}) has been evaluated using electrochemical impedance responses. Figure 4 shows the EIS responses of Zn-Fe coatings on different CDs. It was found that the radii of the distorted semicircles depend on the applied CD for the deposition. At low ACD, a small impedance module was observed at 2 A·dm^{-2} (Figure 2). While at optimal CD (3 A·dm^{-2}), a high impedance module, hence, shows better CR. But at high CD, the impedance module was decreased. Because of the mechanisms of activation at the coating/electrolyte interphase and the diffusion (finite) through the coating thickness, it is evident that the EIS plot (Figure 4) is made of two or more integrated semicircles, and thickness (Table 1) are dependent on the CD as well as the radius of semicircles (impedance of the samples). So, this is consistent with a diffusion-governed mechanism. A simple equivalent circuit is fit at the interface between the coating and the medium. The investigational impedance data at 3.0 A·dm^{-2} was fitted using the ZSimpWin software to the appropriate equivalent circuit model as shown in Figure 5. The estimated values and measured values of the circuit components, namely the inductor (L), capacitor (C), resistor (R), and constant phase element (Q), are found to be in close agreement with experimental data.

3.5 XRD analysis

The CR of the Zn-Fe deposit largely depends on Fe content in the deposit, and hence the change in phase structure is determined by applied CD for the deposition [34,35]. The XRD pattern of Zn-Fe coating at optimal CD (3 A·dm^{-2}) is shown in Figure 4. It may be noted that Zn-Fe alloy electrodeposited at 3.0 A·dm^{-2} displays a relative intensity and position of peaks with face centred cubic lattice structure. The pattern of diffraction peaks appears at an angle of 2θ corresponds to plane lattices with strong peak Zn (103), and the other two peaks are weakly related to Zn (110) and Zn (100) with no extra impurity peaks were related to the secondary phase structure indicates good deposition, residual stresses and texture development can be observed non-destructively. As a result, the phase structure of the coating is severely influenced by the applied CD, which is the fundamental requirement for electrodeposition, and hence the deposit shows better CR (3 A·dm^{-2}) and the diffraction peaks are matched well with the literature. The d-spacing denotes to the distance between adjacent planes of atoms in a crystal lattice. The average crystallite size is 37.87 nm and d spacing is 0.5669 Å from the XRD pattern by estimated using Debye Scherrer formula $D = \frac{K\lambda}{\beta Cos\theta}$ and $d = \frac{\lambda}{2\ Sin\ \theta}$.

Here D is Crystallite size (nm), K will be Scherrer constant (shape factor), λ denotes Wavelength of X-ray diffraction (1.5418 Å), β signifies Full width half maximum (FWHM) in radian, and θ refers to Bragg's angle. The crystallite size and d-spacing were calculated using their respective formulas, and the results are presented in Table 4.

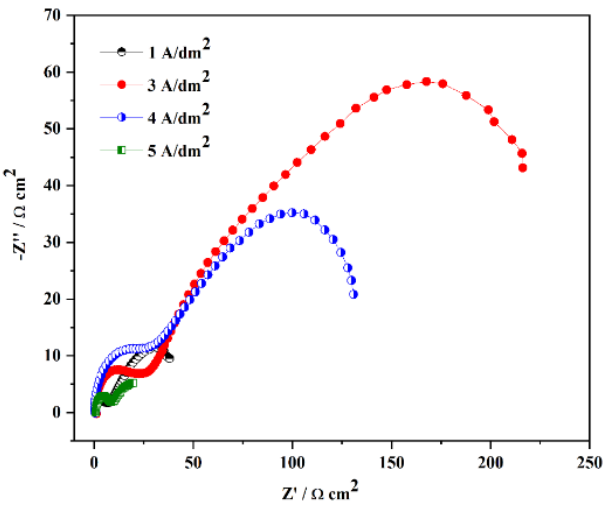

Figure 2. Nyquist plots of Zn-Fe coating films at various ACDs.

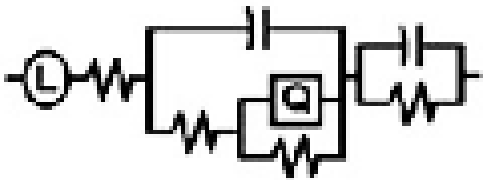

Figure 3. Equivalent circuit model for Zn-Fe coating.

Table 4. The calculated crystallite size, d-spacing, micro-strain and FWHM values.

2θ	FWHM	hkl	Crystalline Size	d- spacing	Micro strain
42.83137	0.3744	101	28.93366	0.5241	0.0418
70.24217	0.4724	103	49.74633	0.7255	0.0561
44.19070	0.2786	110	39.76432	0.5374	0.3294
38.53524	0.3071	100	33.07178	0.4803	0.0694
Average			37.87902	0.5669	0.1033

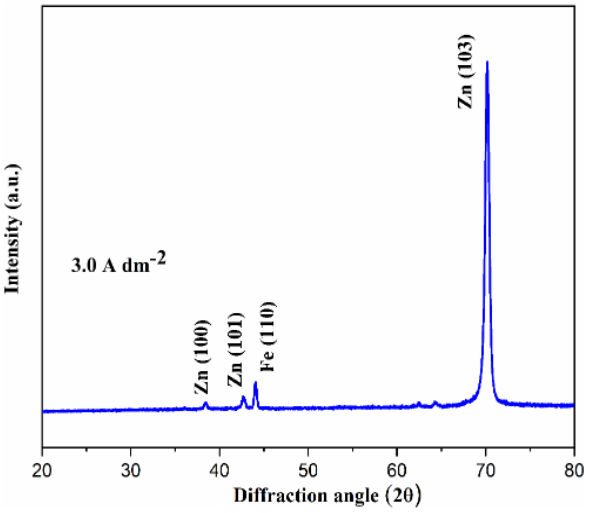

Figure 4. X-ray diffraction patterns of Zn-Fe deposit at optimal CD (3 A·dm^{-2}).

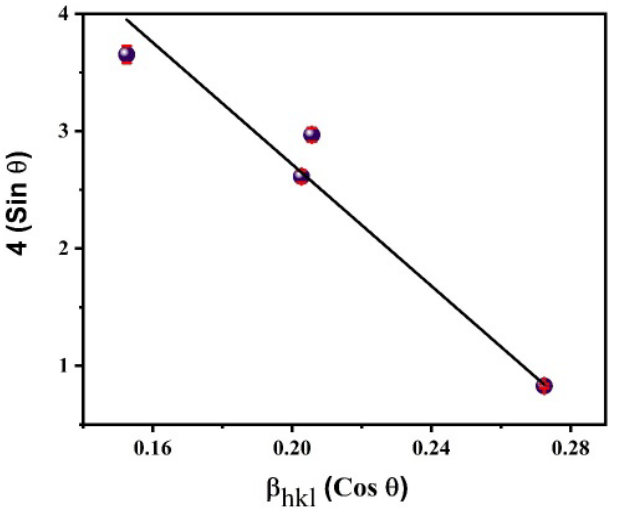

Figure 5. W-H Plot for Zn-Fe alloy coating at optimized current density (3.0 A·dm^{-2}).

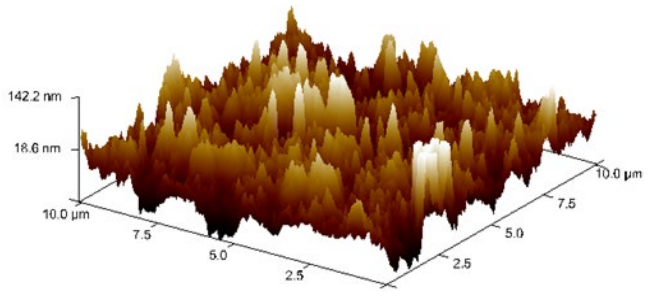

Figure 6. AFM image of Zn-Fe alloy coating (3.0 A·m^{-2}).

3.6 Williamson-Hall (W-H) analysis

Williamson-Hall (W-H) analysis is employed to study the relationship between crystallite size and micro-strain, providing insights into the microstructure of the sample. This method estimates the strain and size from XRD patterns. The W-H plot is constructed by plotting 4 sinθ on the x-axis and $\beta_{hkl}\cos\theta$ on the y-axis, as shown in Figure 5. A straight-line W-H plot indicates a uniform distribution of crystallite size and micro-strain.

$$\beta_{hkl} = \beta_d + \beta_s$$

$$\beta_{hkl}\mathrm{Cos}\theta = \frac{k\lambda}{D} + 4\epsilon\mathrm{Sin}\theta$$

where, β_{hkl} is FWHM of Bragg's peak, β_d related to crystalline size, β_s signifies micro-strain, ϵ refers to micro-strain average. The X-ray line profile for the Zn-Fe coating at the optimal current density (3 A·dm^{-2}) can be analyzed to determine the crystallite size and micro-strain.

3.7 Surface properties

Figure 6 shows a 3D topographical AFM image of a Zn-Fe deposit at 3 A·dm^{-2}. AFM image was used to calculate the root-mean-square roughness (Z_{rms}) and roughness (Ra) of the coatings. The Ra and Z_{rms} values were observed to be 51.1 nm and 66.2 nm. As a result, the examined Zn-Fe electrodeposition was found to be less coarse, and homogeneous, with little peaks (rod) of regular granule size, resulting in better CR (Figure 6).

The 1,2,4 triazole was preferentially absorbed into the Zn-Fe coating matrix, resulting in a lower reduction of Zn^{+2} and Fe^{+2} ions on the matrices, which results in even, crack-free, and homogenous deposits [35] and therefore improved CR. The results of the surface study (AFM and micro-hardness) show that the two primary parameters of coating thickness, the addition of 1,2,4 triazole have a greater impact on the surface microhardness than the topographic grain size of the coatings [36-40]. Figure 7(a-c), are the difference in surface structure because of the deposition CD. It was observed from SEM, that the deposit is non-uniform with a dull appearance (Figure 7(a)) at low CD. The crack-free, smooth, and bright (Figure 7(b)) of coating was found at optimal CD (3.0 A·dm^{-2}) and the formation of the micro pore-free coating on the surface of the substrate acts as a barrier in the penetration of corrosive agents and improves CR. At high CD (5.0 A·dm^{-2}), the surface morphology changed from rough and spherical clusters (Figure 7(c)). Hence, the brightness and uniformity mainly depend on applied CD, and Fe contents in the deposit, and hence changes the phase structure. EDS (Figure 8) confirms the presence of Zn (97.02%), and Fe (2.98%), in the deposit at 3 A·dm^{-2}.

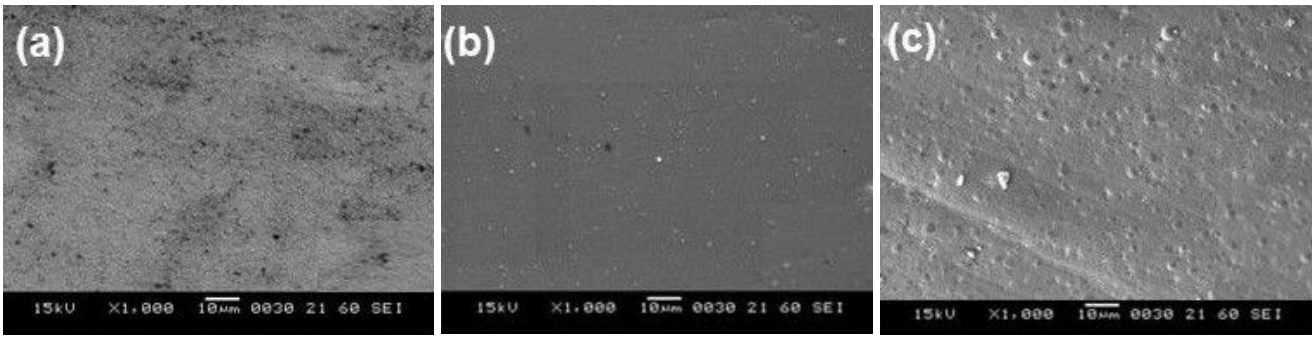

Figure 7. SEM micrographs of Zn-Fe films produced at various ACDs: (a) 1.0 A·dm^{-2}, (b) 3.0 A·dm^{-2}, and (c) 5.0 A·dm^{-2}.

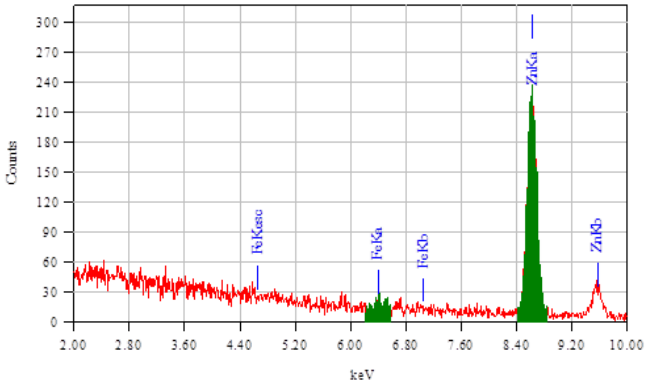

Figure 8. Composition of elements from EDS analysis.

4. Conclusion

A stable electroplating bath for Zn-Fe alloy coatings on MS substrates was developed, incorporating 1,2,4-triazole as an additive to enhance the uniformity and brightness of the coating. In practical applications, the bath showed irregular co-deposition, with zinc preferentially depositing over iron. The Zn-Fe coating, produced at a current density (CD) of 3.0 A·dm^{-2}, contains approximately 3.10 wt% Fe demonstrated the highest corrosion resistance (CR) compared to coatings developed at other CDs. EIS analysis indicated that the enhanced CR at the optimal CD is due to the dielectric barrier properties of the coating layer. XRD analysis identified Zn (100), Zn (101), and Zn (103) reflections, which contribute to the improved CR of the coatings. The surface topography of the deposit at the ideal CD was found to be smooth and intact, further enhancing CR. In conclusion, Zn-Fe alloy coatings show significant potential for applications in the automotive industry, including machinery tools and other components requiring superior corrosion protection.

References

[1] J. Mackowiak, and N. R. Short, "Metallurgy of galvanized coatings," *International Metals Review*, vol. 1, pp. 1-19, 1979.

[2] T. V. Byk, T. V. Gaevskaya, and L. S. Tsybulskaya, "Effect of electrodeposition conditions on the composition, microstructure, and corrosion resistance of Zn-Ni alloy coatings," *Surface and Coatings Technology*, vol. 202, pp. 5817-5823, 2008.

[3] A. Tozar, and I. H. Karahan, "Structural and corrosion protection properties of electrochemically deposited nano-sized Zn-Ni alloy coatings," *Applied Surface Science*, vol. 318, pp. 15-23, 2014.

[4] A. P. Yadav, H. Katayama, K. Noda, H. Masuda, A. Nishikata, and T. Tsuru, "Effect of Fe-Zn alloy layer on the corrosion resistance of galvanized steel in chloride-containing environments," *Corrosion Science*, vol. 49, pp. 3716-3731, 2007.

[5] Z. Zhang, W. H. Leng, H. B. Shao, J. Q. Zhang, J. M. Wang, and C. N. Cao, "Study on the behavior of Zn–Fe alloy electroplating," *Journal of Electroanalytical Chemistry*, vol. 516, pp. 127-130, 2001.

[6] M. H. Gharahcheshmeh, and M. H. Sohi, "Study of the corrosion behavior of zinc and Zn-Co alloy electrodeposits obtained from the alkaline bath using direct current, *Materials Chemistry and Physics*, vol. 2, pp. 414-421, 2009.

[7] M. M. Abou-Krishna, and A. M. Abushoffa, "Stripping voltammetric, conductance, and anodic linear polarization analysis on dissolution of electrodeposited zinc-cobalt alloy," *International Journal of Electrochemical Science*, vol. 5, pp. 418-432, 2007.

[8] J. B. Bajat, S. Stankovic, and B. M. Jokic, "Electrochemical deposition, and corrosion stability of Zn–Co alloys," *Journal of Solid State Electrochemistry*, vol. 13, pp. 755-762, 2009.

[9] R. S.Bhat, and V. B. Shet, "Development and characterization of Zn-Ni, Zn-Co, and Zn-Ni-Co coatings," *Surface Engineering*, vol. 36, pp. 429-437, 2020.

[10] K. Venkatakrishna, A. C Hegde, and N. Eliaz, "Electrodeposition of bright Zn-Fe alloy on mild steel from acid chloride bath," *Indian Journal of Materials Science*, vol. 5, pp. 289-298, 2009.

[11] R. Ramanauskas, R. Juskenas, L. Kalinicenko, and F. Garfias-Mesias, "Microstructure, and corrosion resistance of electrodeposited zinc alloy coatings," *Journal of Solid State Electrochemistry*, vol. 8, pp. 416-421, 2004.

[12] C. Q. Yang, Z. L. Long, and Y. C. Zhou, "Electrodeposition and physicochemical properties of Zn-Fe alloy coatings from sulfate solution," *Journal of Materials Science Letters*, vol. 21, pp. 1677-1680, 2002.

[13] De Carvalho MF, E. P. Barbano, and I. A. Carlos, "Influence of disodium ethylene diamine tetraacetate on zinc electrodeposition process and the morphology, chemical composition, and structure of the electrodeposits," *Electrochimica Acta*, vol. 109, pp. 798-808, 2013.

[14] R. Bhat, U. K Bhat, and A. C. Hegde, "Optimization of deposition conditions for bright Zn-Fe coatings and its characterization,"

Protection of Metals and Physical Chemistry of Surfaces, vol. 47, pp. 645-653, 2011.

[15] T. Boiadjieva-Scherzer, G. Avdeev, T. Vassilev, V. Chakarova, H. Kronberger, and M. Monev, "Influence of annealing temperature on ζ-$CrZn_{13}$ formation in electrodeposited Zn–Cr coatings," *Surface Engineering*, vol. 35, pp. 1055-1060, 2020.

[16] C. Oulmas, S. Mameri, D. Boughrara, A. Kadri, J. Delhalle, Z. Mekhalif, and B. Benfedda, "Comparative study of Cu-Zn coatings electrodeposited from sulphate and chloride baths," *Heliyon*, vol. 5, p. 02058, 2019.

[17] M. M. Abou-Krisha, A. M. Zaky, and A. A. Toghan, "Morphology, composition, and corrosion properties of electro-deposited Zn-Ni alloys from sulphate electrolytes," *Asian Journal of Biochemistry*, vol. 1, pp. 84-97, 2006.

[18] Y. T. Hsieh, R. W. Tsai, C. J. Su, and L. W. Sun, "Electro-deposition of Cu-Zn from chlorozincate ionic liquid: From hollow tubes to segmented nanowires, *Journal of Physical Chemistry C*, vol. 118, pp. 22347-22355, 2014.

[19] M. M. Abou-Krisha, F. H. Assaf, and A. A. Toghan, "Electro deposition of Zn-Ni alloys from sulfate bath," *Journal of Solid State Electrochemistry*, vol. 11, pp. 244-252, 2007.

[20] R. Solmaz, and B. D. Karahan, "Characterization, and corrosion studies of ternary Zn-Ni-Sn alloys," *International Journal of Minerals, Metallurgy and Materials*, vol. 1, pp. 74-82, 2020.

[21] R. S. Bhat, U. Bhat, and A. C. Hegde, "Corrosion behavior of electrodeposited Zn-Ni, Zn-Co, and Zn-Ni-Co alloys," *Analytical and Bioanalytical ElectroChemistry*, vol. 3, pp. 302-315, 2011.

[22] N. Eliaz, K. Venkatakrishna, and A. C. Hegde, "Electroplating and characterization of Zn-Ni, Zn-Co, and Zn-Ni-Co alloys," *Surface and Coatings Technology*, vol. 205, pp. 1969-1978, 2010.

[23] A. Toghan, M. M. Abou-krisha, F. H. Assaf, and F. El-Sheref, "Effect of deposition potential on the mechanism and corrosion behavior of Zn-Fe-Co thin coatings electrochemically deposited on a steel substrate," *International Journal of Electrochemical Science*, vol. 16, p. 151044, 2021.

[24] A. R. Marder, "The metallurgy of zinc-coated steel, *Progress in Materials Science*, vol. 45, pp. 191-271, 2000.

[25] K. R. Sriraman, S. Brahimi, J. A. Szpunar, J. H. Osborne, and S. Yue, "Characterization of corrosion resistance of electro-deposited Zn-Ni Zn and Cd coatings, *Electrochimica Acta*, vol. 105, pp. 314-323, 2013.

[26] T. Y. Soror, and M. A. El-Ziady, "Effect of cetyl trimethyl ammonium bromide on the corrosion of carbon steel in acids," *Materials Chemistry and Physics*, vol. 77, pp. 697-703, 2003.

[27] A. I . Vogel, "Quantitative inorganic analysis," Longmans Green and Co., London,1951.

[28] A. Brenner, "Electrodeposition of alloys," Academic Press, New York, vol. 2, pp. 194, 1963.

[29] R. S. Bhat, S. M. Shetty, and N. V. Anil Kumar, "Electroplating of Zn-Ni alloy coating on mild steel and its electrochemical studies, *Journal of Materials Engineering and Performance*, vol. 30, pp. 8188-8195, 2021.

[30] R. S. Bhat, K. B. Manjunatha, R. Prasanna Shankara, K. Venkatakrishna, and A. C. Hegde, "Electrochemical studies on the corrosion resistance of Zn-Ni-Co coating from acid chloride bath," *Applied Physics A*, vol. 126, pp. 772, 2020.

[31] A. Tozar, and I. H. Karahan, "Structural and corrosion protection properties of electrochemically deposited nano-sized Zn-Ni alloy coatings," *Applied Surface Science*, vol. 318, pp. 15-23, 2014.

[32] J. B. Bajat, M. D. Maksimovic, V. B. Miskovic-Stankovic, and S. Zec, "Electrodeposition and characterization of Zn-Ni alloys as sublayers for epoxy coating deposition," *Journal of Applied Electrochemistry*, vol. 31, pp. 355-361, 2001.

[33] A. Petrauskas, L. Grinceviciene, A. Cesuniene, and R. Juskenas, "Influence of Co^{2+} and Cu^{2+} on the phase composition of Zn-Ni alloys," *Electrochimica Acta*, vol. 51, pp. 6135-6139, 2006.

[34] J. B. Bajat, and V. B. Miskovic-Stankovic, "Protective properties of epoxy coatings electrodeposited on steel electrochemically modified by Zn-Ni alloys," *Progress in Organic Coatings*, vol. 49, pp. 183-186, 2004.

[35] M. M. Younan, "Surface microstructure and corrosion resistance of electrodeposited ternary Zn-Ni-Co alloy," *Journal of Applied Electrochemistry*, vol. 30, pp. 55-60, 2000.

[36] A. T. Tabrizi, H. Aghajani, and F. F. Lelah, "Tribological characterization of hybrid chromium nitride thin layer synthesized on titanium," *Surface and Coatings Technology*, vol. 15, p. 127317, 2021.

[37] M. Delaram, A. T. Tabrizi, and H. Aghajani, "Study the variation of surface topography & corrosion resistance of Cr-GO nano-composite coatings by addition of GO nanoparticles," *Surface Topography: Metrology and Properties*, vol. 9, p. 015025, 2021.

[38] Y. Lin, and J. Selman, "Electrodeposition of corrosion-resistant Ni-Zn alloy: I. Cyclic voltammetric study," *Electrochemical Society*, vol. 140, p. 1299, 1993.

[39] Z. Feng, Q. Li, J. Zhang, P. Yang, H. Song, and M. An, "Electro-deposition of nanocrystalline Zn–Ni coatings with single gamma phase from an alkaline bath," *Surface and Coatings Technology*, vol. 47, p. 270, 2015.

[40] Z. Feng, Q. Li, J. Zhang, P. Yang, and M. An, "Experimental and theoretical studies of DMH as a complexing agent for a cyanide-free gold electroplating electrolyte," *RSC Advances*, vol. 5, p. 58199, 2015.